Scientific Paper

Perturbation Density Functional Theory for Inhomogeneous Fluids†

Shiqi Zhou[a] and Andrej Jamnik[b]

[a]*Institute of Modern Statistical Mechanics, Hunan, University of Tehcnology, Wenhua Road, Zhuzhou city, 412008, P. R. China*

[b]*University of Ljubljana, Faculty of Chemistry and Chemical Technology, Aškerčeva 5, SI-1001 Ljubljana, Slovenia*

Received 10-04-2006

† Dedicated to the memory of Prof. Dr. Davorin Dolar

Abstract

A recently developed third order+second order perturbation density functional approximation (DFA) is briefly described. The applicability of this theory is demonstrated in the study of the density profiles of Lennard-Jones (LJ) fluid next to a large hard sphere (mimicking a colloidal particle) of various sizes. The accuracy of DFA predictions is tested against the results of a grand canonical ensemble Monte Carlo simulation. The chosen density and potential parameters for the equilibrium bulk LJ fluid correspond to the conditions situated at 'dangerous' regions of the phase diagram, i.e. near the critical temperature or close to the gas-liquid coexistence curve. It is found that the DFA theory performs successfully for both supercritical and subcritical temperatures. It is also shown that the 'universality' of the adjustable parameter associated with this theory holds also in the present case of a large spherical particle as a source of external potential. Here the term universality means independence of this parameter on the particular external field responsible for the generation of a non-uniform density profile of the fluid. This DFA results can be used as a useful starting point for further investigation of solvent-induced excess potential of mean force in the similar systems.

Key words: perturbation density functional theory, Monte Carlo simulation, inhomogeneous systems

1. Introduction

A powerful theoretical tool for the calculation of the inhomogeneous fluid structure is the so-called density functional theory (DFT),[1] which was introduced into the classical statistical mechanics since more than four decades.[2] The classical DFT has also its quantum counterpart (quantum DFT), originally devised for the simplified solution of the complicated quantum many-body problems.[3] During the time since its development, four main methodologies of the classical DFT have been evolved. One such version is the functional perturbation expansion approximation[4] (FPEA) for the excess free energy of the non-uniform system around that of the homogeneous system in powers of the density deviation between the non-uniform density distribution and bulk density. The coefficients at this expansion represent the direct correlation functions (DCFs) of the uniform system. In most of the early studies, this expansion was truncated at the second order due to the lack of the knowledge of the higher order DCFs even for the uniform bulk fluid. In a recent study,[5] higher order expansion approximation has been developed by making use of approximate higher order DCFs. A new version of the FPEA, which is also of second order but actually including a content of the higher orders, is the so-called Lagrangian theorem-based DFA (LTDFA)[6] and its free version comprising an adjustable parameter.[7] Another type of DFT is the so-called weighted density approximation[1] (WDA) and its various variants,[8] which are actually mappings of non-uniform systems into uniform counterparts and include approximate contributions to the free energy density functional from all orders in density difference. In the WDA approach, the excess free energy or its functional derivative (the first order DCF) of the non-uniform fluids are approximated by those of the corresponding uniform fluid at a smoothed average density, which is actually a suitable weighted average of the physical density of the system under consideration. The third variety of DFT is the fundamental measure theory proposed by Rosenfeld.[9] It is based on geometrical considerations and specifies the excess free energy by reproducing the Percus-Yevick (PY) equation of state and the PY second order DCF of the hard sphere fluid. Recently, the fourth kind of DFT has been proposed.[10]

It uses the concept of the universality of the free energy density functional and collects all of the higher orders beyond the second order of the functional perturbation expansion in the form of bridge functional. All of these versions of the DFT were originally devised for non-uniform hard sphere fluid. However, their extensions to non-hard sphere models represent different stories. Briefly speaking, these extensions[1] treat the tail part of the interaction potential by mean field approximation and the hard-core part by the hard sphere DFA, the two exceptions being the universal theoretical way[11] and the so-called third order+second order perturbation DFA[12] proposed by one of the present authors. It was shown[13] that the latter theory performs well on condition of the high reliability of the imported bulk second order DCF. A key problem associated with this theory is the use of an adjustable parameter. In a series of our previous works,[13,14] we determined this parameter by employing the single hard wall sum rule and then used the same value of this parameter also for other external fields that considerably deviated from that imposed by a single wall. In this way we found a 'transplant' property of the adjustable parameter in a sense of its applicability for any inhomogeneous environment, which has been denoted as a 'universality' of this parameter.

The aim of the present investigation is to test the universality of the adjustable parameter and to give a judgment about the validity and the applicability of the third order+second order perturbation DFA in predicting the inhomogeneous structure of a prototype model fluid. For the latter we have chosen the Lennard-Jones (LJ) model, which has been the most frequently applied to model the attractive dispersion forces in a variety of physical situations ranging from the simplest case of modeling the interactions in simple fluids to much more complex systems including solvent averaged interactions in colloidal suspensions. This model has been especially popular also as the sample model used for critical tests of statistical mechanical theories. In our previous paper,[14] LJ model was used to estimate the accuracy of the third order+second order perturbation density functional approximation (DFA) in predicting the structure of this fluid subjected to diverse external fields stemming from the presence of various spatial constrains reflecting various degree of confinement. For the latter, we have chosen a hard flat interface, a planar slit consisting of two parallel, perfectly smooth hard walls, and a closed spherical surface mimicking a spherical cavity. DFA predictions were tested against the results of a grand canonical ensemble Monte Carlo (GCEMC) simulation. In the present work, we report on an analogous study of the structure of LJ fluid around a large hard sphere of different sizes mimicking an inhomogeneous system formed by single spherical colloidal particle immersed in a LJ solvent. Apart from the primary goal of the present work, i.e. the critical test of the theoretical method, this investigation is significant also from the view of the model used. Namely, the theoretical study of the structural and related thermodynamic properties of asymmetric fluid mixtures is very important for understanding a variety of problems in colloid chemistry as a colloid dispersion can be modeled as a multicomponent system formed by large (macro)particles mimicking colloidal solute and smaller molecules denoting the solvent component. The determination of the local structure of such inhomogeneous systems has therefore long been the subject of intense theoretical research and numerous studies have reported the results of thermodynamic and structural properties of fluids in the vicinity of macroparticles of different shapes. A particular attention has been paid to the dependence of these properties on the size of colloidal macroparticles. The structure of the molecular solvent in the interface among colloidal particles is also responsible for the intercolloidal solvation force, often called also as solvent mediated or structural force. As colloidal particles take part in various chemical and biological reactions, knowledge of the solvation force is also of great practical importance. For this reason, the present results will also serve as a useful starting point for the further investigation of solvent-induced excess potential of mean force in the similar systems.

2. Model and Methods

2.1. The Model

As in our previous work[14] we consider the Lennard-Jones (LJ) fluid with the potential function

$$u_{lj}(r) = 4\varepsilon\left[\left(\frac{r}{\sigma}\right)^{-12} - \left(\frac{r}{\sigma}\right)^{-6}\right] \qquad (1)$$

where ε and σ are the energy and size parameters of the potential, respectively. In the following the reduced units are used for the absolute temperature T, $T^* = kT/\varepsilon$ with k being the Boltzmann constant.

Further, the interaction among the LJ particles and large spherical particle of effective radius R is a hard core one:

$$\varphi_{ext}(\mathbf{r}) = \infty \qquad |\mathbf{r}| < R$$
$$= 0, \quad \text{elsewhere} \qquad (2)$$

where φ_{ext} denotes the external potential.

2.2. Open Ensemble Simulation

For the LJ model of Eq. (1) we have carried out Grand Canonical Ensemble Monte Carlo (GCEMC) simulations at constant chemical potential μ, volume V, and temperature T. This set of independent parameters that define the thermodynamic state of

the system made possible the study of equilibrium between the bulk LJ fluid and the same fluid subjected to external field originating from the presence of the large spherical particle. The general features of the GCEMC method are described elsewhere.[15] Further, some details peculiar to this study are discussed in our previous work.[14] Therein, the results of independent simulations of the bulk LJ fluid are also presented. Apart from our interest in the bulk interparticle correlations, these simulations were needed to adjust the values of the chemical potential to the desirable bulk densities. Because of the equilibrium, of course, the same values for the chemical potential were then used in the simulation of the present inhomogeneous system, where, similarly as in the case of homogeneous (bulk) phase, the Monte Carlo (MC) cell was a cubic box with the periodic boundary conditions imposed in all three directions. The LJ fluid surrounded a large hard sphere located at the center of the cell. Simulations of the system with bigger central particle requested larger dimensions of MC box to assure distances larger than the distance where correlations between the hard particle from the basic MC cell and its images from the surrounding cells were still detected. In addition, our recent work mentioned above contains also the simulation results for the density profiles of the LJ fluid near a single hard wall. By considering the contact theorem, the value for an adjustable parameter was determined from the corresponding simulation data for each set of the bulk potential and density parameters. This parameter is included in the DFA theory briefly described in the next section.

The liquid-gas phase behavior of the pure LJ fluid was investigated by Potoff and Panagiotopoulos.[16] Using grand canonical MC simulations they determined the liquid-vapor coexistence curve and critical point. The critical parameters of the untruncated LJ potential were assessed as $T_c^* = 1.312$ and $\rho_c^* = 0.316$. We have performed calculations for two reduced temperatures, the value of the first being slightly higher and that of the latter slightly lower than the critical value 1.312. The ratio between the chosen supercritical temperature and the critical value was 1.06. For this regime, a broad range of bulk reduced densities ranging from the value 0.1 to 0.7 has been investigated. The ratio between the chosen subcritical temperature and the critical value was 0.98. For this subcritical regime, however, only narrow 1-phase regions corresponding either to monophasic gaseous state (low densities) or monophasic liquid state (high densities) could be explored. For this reason, there are only a few simulation data presented for this regime.

2.3. Third Order+Scond Order Perturbation Density Functional Theory

In the following we give a concise description of the third order+second order perturbation DFT approach.[13,14] The approximate analytical expression for the bulk third order direct correlation function (DCF) of the hard sphere (HS) fluid is given by[5]

$$C_{0hs}^{(3)}(\mathbf{r},\mathbf{r}_1,\mathbf{r}_2;\rho_b) = \frac{C_{0hs}^{(1)^2}(\rho_b)}{\left[C_{0hs}^{(1)'}(\rho_b)\right]^3}\int C_{0hs}^{(2)}(\mathbf{r}_0,\mathbf{r};\rho_b)\, C_{0hs}^{(2)}(\mathbf{r}_0,\mathbf{r}_1;\rho_b)\, C_{0hs}^{(2)}(\mathbf{r}_0,\mathbf{r}_2;\rho_b)\, d\mathbf{r}_0 \tag{3}$$

where the subscript 'hs' denotes the quantities for the HS fluid. Throughout the text, superscript (n) denotes the corresponding n-order quantities; absence of the subscript 0 refers to non-uniform case, while the presence of the subscript 0 refers to the uniform system. Functional perturbation expansion of the non-uniform first order DCF $C_{hs}^{(1)}(\mathbf{r};[\rho])$ for HS fluid around the equilibrium bulk density ρ_b leads to the expression

$$C_{hs}^{(1)}(\mathbf{r};[\rho]) = C_{0hs}^{(1)}(\rho_b) + \int d\mathbf{r}_1 (\rho(\mathbf{r}_1)-\rho_b)\, C_{0hs}^{(2)}(|\mathbf{r}-\mathbf{r}_1|;\rho_b) + \sum_{n=3}^{\infty}\frac{1}{(n-1)!}\int d\mathbf{r}_1 \int d\mathbf{r}_2 \cdots \int d\mathbf{r}_{n-1}\prod_{m=1}^{n-1}[\rho(\mathbf{r}_m)-\rho_b]\, C_{0hs}^{(n)}(\mathbf{r},\mathbf{r}_1,\cdots,\mathbf{r}_{n-1};\rho_b) \tag{4}$$

Discarding away all of the terms with n<3 in the sum of Eq. (4) then yields

$$C_{hs}^{(1)}(\mathbf{r};[\rho]) = C_{0hs}^{(1)}(\rho_b) + \int d\mathbf{r}_1 (\rho(\mathbf{r}_1)-\rho_b)\, C_{0hs}^{(2)}(|\mathbf{r}-\mathbf{r}_1|;\rho_b) + \frac{1}{2}\int d\mathbf{r}_1 \int d\mathbf{r}_2 \prod_{m=1}^{2}[\rho(\mathbf{r}_m)-\rho_b]\, C_{0hs}^{(3)}(\mathbf{r},\mathbf{r}_1,\mathbf{r}_2;\rho_b) \tag{5}$$

Combination of Eqs. (3) and (5) leads to the so-called hard sphere third order perturbation DFT approach

$$C_{hs}^{(1)}(\mathbf{r};[\rho]) = C_{0hs}^{(1)}(\rho_b) + \int d\mathbf{r}'[\rho(\mathbf{r}')-\rho_b]\, C_{0hs}^{(2)}(|\mathbf{r}-\mathbf{r}'|;\rho_b) + \frac{C_{0hs}^{(1)''}(\rho_b)}{2\left[C_{0hs}^{(1)'}(\rho_b)\right]^3}\int C_{0hs}^{(2)}(\mathbf{r},\mathbf{r}'';\rho_b)\left[\int C_{0hs}^{(2)}(\mathbf{r}',\mathbf{r}'';\rho_b)(\rho(\mathbf{r}')-\rho_b)\, d\mathbf{r}'\right]^2 d\mathbf{r}'' \tag{6}$$

In the framework of the partitioned DFT formalism[12,17] one splits the bulk second order DCF $C_0^{(2)}(r;\rho_b\cdots)$ into the hard-core part $C_{0hc}^{(2)}(r;\rho_b\cdots)$ and tail part $C_{0tail}^{(2)}(r;\rho_b\cdots)$:

$$C_0^{(2)}(r;\rho_b\cdots)=C_{0hc}^{(2)}(r;\rho_b\cdots)+C_{0tail}^{(2)}(r;\rho_b\cdots) \quad (7)$$

where

$$\begin{aligned} C_{0hc}^{(2)}(r;\rho_b\cdots) &= C_0^{(2)}(r;\rho_b\cdots) && r<r_{cut} \\ &= 0 && r>r_{cut} \end{aligned} \quad (8)$$

and

$$\begin{aligned} C_{0tail}^{(2)}(r;\rho_b\cdots) &= 0 && r<r_{cut} \\ &= C_0^{(2)}(r;\rho_b\cdots) && r>r_{cut} \end{aligned} \quad (9)$$

Further, we have similarly:

$$C^{(1)}(\mathbf{r};[\rho]\cdots)=C_{hc}^{(1)}(\mathbf{r};[\rho]\cdots)+C_{tail}^{(1)}(\mathbf{r};[\rho]\cdots) \quad (10)$$

and

$$C_0^{(1)}(\rho_b\cdots)=C_{0hc}^{(1)}(\rho_b\cdots)+C_{0tail}^{(1)}(\rho_b\cdots) \quad (11)$$

Here, the set $\rho_b\cdots$ stands for the bulk density and potential parameters. The tail part $C_{0tail}^{(2)}(r;\rho_b\cdots)$ is usually only weakly dependent on the density argument.[12,17,18] This allows the tail part $C_{tail}^{(1)}(\mathbf{r};\rho_b\cdots)$ of the non-uniform first order DCF to be treated by the second order functional perturbation expansion approximation (FPEA)

$$C_{tail}^{(1)}(\mathbf{r};[\rho]\cdots)=C_{0tail}^{(1)}(\rho_b\cdots)+\int d\mathbf{r}_1(\rho(\mathbf{r}_1)-\rho_b)\,C_{0tail}^{(2)}(|\mathbf{r}-\mathbf{r}_1|;\rho_b\cdots) \quad (12)$$

For the hard-core part, one can directly apply the so-called hard sphere third order perturbation DFT approach comprised in Eq. (6). Here, the term 'directly' is used in a sense of a direct substitution of the quantities for HS fluid by the corresponding quantities for hard-core part in hard sphere third order perturbation DFT approach. After applying the Eq. (6) to hard-core part, one has

$$\begin{aligned} C_{hc}^{(1)}(\mathbf{r};[\rho]\cdots)=&C_{0hc}^{(1)}(\rho_b\cdots)+\int d\mathbf{r}'[\rho(\mathbf{r}')-\rho_b]\,C_{0hc}^{(2)}(|\mathbf{r}-\mathbf{r}'|;\rho_b\cdots) \\ &+\frac{C_{0hc}^{(1)''}(\rho_b\cdots)}{2\left[C_{0hc}^{(1)'}(\rho_b\cdots)\right]^3}\int C_{0hc}^{(2)}(\mathbf{r},\mathbf{r}'';\rho_b\cdots)\left[\int C_{0hc}^{(2)}(\mathbf{r}',\mathbf{r}'';\rho_b\cdots)(\rho(\mathbf{r}')-\rho_b)d\mathbf{r}'\right] \end{aligned} \quad (13)$$

Further, a combination of Eqs. (7-13) leads to

$$\begin{aligned} C^{(1)}(\mathbf{r};[\rho]\cdots)=&C_0^{(1)}(\rho_b\cdots)+\int d\mathbf{r}'\,[\rho(\mathbf{r}')-\rho_b]\,C_{0hc}^{(2)}(|\mathbf{r}-\mathbf{r}'|;\rho_b\cdots)+ \\ &+\frac{C_{0hc}^{(1)''}(\rho_b\cdots)}{2\left[C_{0hc}^{(1)'}(\rho_b\cdots)\right]^3}\int C_{0hc}^{(2)}(\mathbf{r},\mathbf{r}'';\rho_b\cdots)\left[\int C_{0hc}^{(2)}(\mathbf{r}',\mathbf{r}'';\rho_b\cdots)(\rho(\mathbf{r}')-\rho_b)d\mathbf{r}'\right]^2 d\mathbf{r}'' \\ &+\int d\mathbf{r}_1(\rho(\mathbf{r}_1)-\rho_b)\,C_{0tail}^{(2)}(|\mathbf{r}-\mathbf{r}_1|;\rho_b\cdots) \\ =&C_0^{(1)}(\rho_b\cdots)+\int d\mathbf{r}'[\rho(\mathbf{r}')-\rho_b]\,C_0^{(2)}(|\mathbf{r}-\mathbf{r}'|;\rho_b\cdots) \\ &+\frac{C_{0hc}^{(1)''}(\rho_b\cdots)}{2\left[C_{0hc}^{(1)'}(\rho_b\cdots)\right]^3}\int C_{0hc}^{(2)}(\mathbf{r},\mathbf{r}'';\rho_b\cdots)\left[\int C_{0hc}^{(2)}(\mathbf{r}',\mathbf{r}'';\rho_b\cdots)(\rho(\mathbf{r}')-\rho_b)d\mathbf{r}'\right]^2 d\mathbf{r}'' \end{aligned} \quad (14)$$

The coefficient $\dfrac{C_{0hc}^{(1)''}(\rho_b\cdots)}{2\left[C_{0hc}^{(1)'}(\rho_b\cdots)\right]^3}$ in the last Eq. (14) is used as an adjustable parameter denoted by λ. Then we finally have:

$$\begin{aligned} C^{(1)}(\mathbf{r};[\rho]\cdots)=&C_0^{(1)}(\rho_b\cdots)+\int d\mathbf{r}'[\rho(\mathbf{r}')-\rho_b]\,C_0^{(2)}(|\mathbf{r}-\mathbf{r}'|;\rho_b\cdots) \\ &+\lambda(\rho_b\cdots)\int C_{0hc}^{(2)}(\mathbf{r},\mathbf{r}'';\rho_b\cdots)\left[\int C_{0hc}^{(2)}(\mathbf{r}',\mathbf{r}'';\rho_b\cdots)(\rho(\mathbf{r}')-\rho_b)d\mathbf{r}'\right]^2 d\mathbf{r}'' \end{aligned} \quad (15)$$

Combination of Eq. (15) and the expression for the single component density profile given by

$$\rho(\mathbf{r})=\rho_b\exp\left\{-\beta\varphi_{ext}(\mathbf{r})+C^{(1)}(\mathbf{r};[\rho]\cdots)-C_0^{(1)}(\rho_b\cdots)\right\} \quad (16)$$

can be used to predict the density profile of the single component atomic fluid subjected to diverse external fields. Here $\varphi_{ext}(\mathbf{r})$ is the external potential responsible for the generation of the inhomogeneous spatial density distribution $\rho(\mathbf{r})$. In the present work the above Eqs. (15) and (16) are applied for the calculation of the

density profiles of LJ fluid under the influence of external potential denoted by Eq. (2). The LJ potential is truncated and shifted at r_c as done in the simulation, the resultant potential $u_{lj}^{ts}(r)$ is given by

$$\begin{aligned} u_{lj}^{ts}(r) &= u_{lj}(r) - u_{lj}(r_c) && r \le r_c \\ &= 0 && r \ge r_c \end{aligned} \qquad (17)$$

The required bulk second order DCF $C_0^{(2)}(r;\rho_b\cdots)$ is obtained numerically from the OZ integral equation

$$\gamma(r) = h(r) - C_0^{(2)}(r;\rho_b\cdots) = \rho_b \int d\mathbf{r}_1 h(\mathbf{r}_1)\, C_0^{(2)}(|\mathbf{r}-\mathbf{r}_1|;\rho_b\cdots) \qquad (18)$$

along with the closure relation

$$h(r) + 1 = \exp\{-u_{lj}^{ts}(r) + \gamma + B(s)\} \qquad (19)$$

Above, $s = \gamma(r) - \beta u_2(r)$ is the so-called renormalization indirect correlation function and B is the bridge functional specified as follows:

$$\begin{aligned} B(s) &= \frac{-s^2}{2[1+0.8s]} && s \ge 0 \\ &= -0.5s^2 && s < 0 \end{aligned} \qquad (20)$$

The bridge functional, Eq. (20), is obtained by substituting a well-known VM bridge functional with $-0.5s^2$ for $s < 0$,[19] and leaving it unchanged for $s \ge 0$. The expression for the perturbation part of the potential $\beta u_2(r)$ is taken from the Ref. 20. The adjustable parameter λ we determine by a single hard wall sum rule, similarly as done in our previous works on hard-core attractive Yukawa (HCAY) fluid[13] and LJ fluid.[14]

First, the adjustable parameter λ for each set of parameters of the coexistence bulk fluid is determined by the single hard wall sum rule. The pressure of the equilibrium bulk fluid required for this purpose is obtained by considering the contact theorem relating the pressure and the single hard wall contact density. For the latter we utilize the exact simulation result, the pressure being equal to $\rho(0.5\sigma)/\beta$. This means that the parameter λ is adjusted to the value ensuring the equality of the single hard wall contact density predicted by the present DFT approach and that obtained by 'exact' simulation method. Because of the universality of the adjustable parameter λ one can use the same numerical value obtained from the single hard wall case also for other external potentials, here the one originating from the presence of a single large hard sphere, Eq. (2).

3. Numerical Results and Discussion

In Figures 1 and 2 the GCEMC and DFT results for the density profiles of the LJ fluid near large hard spheres in equilibrium with the bulk fluid are compared. The corresponding values for the adjustable parameter λ, obtained for each temperature and bulk density, are also presented. Calculations were performed for two reduced temperature: at supercritical temperature $1.06 \cdot T_c^*$ (Figure 1) and at subcritical temperature $0.98 \cdot T_c^*$ (Figure 2). For the supercritical regime, the values of the bulk reduced density cover a broad range from 0.1 to 0.7. Subcritical regime, however, is represented by only two values of the bulk density lying in narrow 1-phase regions of the phase diagram corresponding either to monophasic gaseous state (low density) or monophasic liquid state (high density). Three different sizes of the hard sphere are considered: the largest one with the radius $R' = 5\sigma$, a relatively small sphere of $R' = 1\sigma$, and one of intermediate size $R' = 2\sigma$. The centers of the particles of LJ fluid are therefore constrained to the distances $r > R = (R' + \sigma/2)$. Both figures contain parts (a)-(c), which successively illustrate the effect of the increasing of the size of the large sphere.

A careful inspection of the presented local structures around the hard spherical body leads to a conclusion that the DFT predictions excellently agree with the simulation results. Except at the large sphere/fluid contact surface and its immediate vicinity, the DFT density profiles agree quantitatively with the simulation data. Both methods predict distinct density oscillations in the domain close to the surface of the large particle revealing important packing effects due to the finite size (excluded volume) of the molecules of the fluid. Of course, the amplitude of the oscillations depends on the density of the equilibrium bulk fluid and also on the temperature of the system. At higher temperature, the attraction among the molecules loses in importance in comparison with their thermal energy. Such molecules thus resemble the hard (repulsive) particles that, due to the steric shielding effects, tend to accumulate adjacent to the boundary of the constraint thus giving rise to higher contact values and more pronounced oscillations of the local density. Upon reducing temperature, the role of the attractive part in the intermolecular potential of interaction increases causing an efficient competition of interparticle attraction with the steric effects. In this case, the strongly attractive molecules try to avoid the region near the hard sphere as they have a better chance for mutual attraction at sufficient distances from the repulsive constraint. This leads to a reduction of the contact density and amplitude of the oscillations that gradually disappear. As noted above, the agreement between the theory and simulation is excellent except in close vicinity of the hard sphere/fluid contact plane where a slight deviation can be observed. As expected, this deviation slightly increases upon the reducing the size of large sphere as the performance of the theory should improve with increasing the size of the macroparticles. Finally, it should do the best job

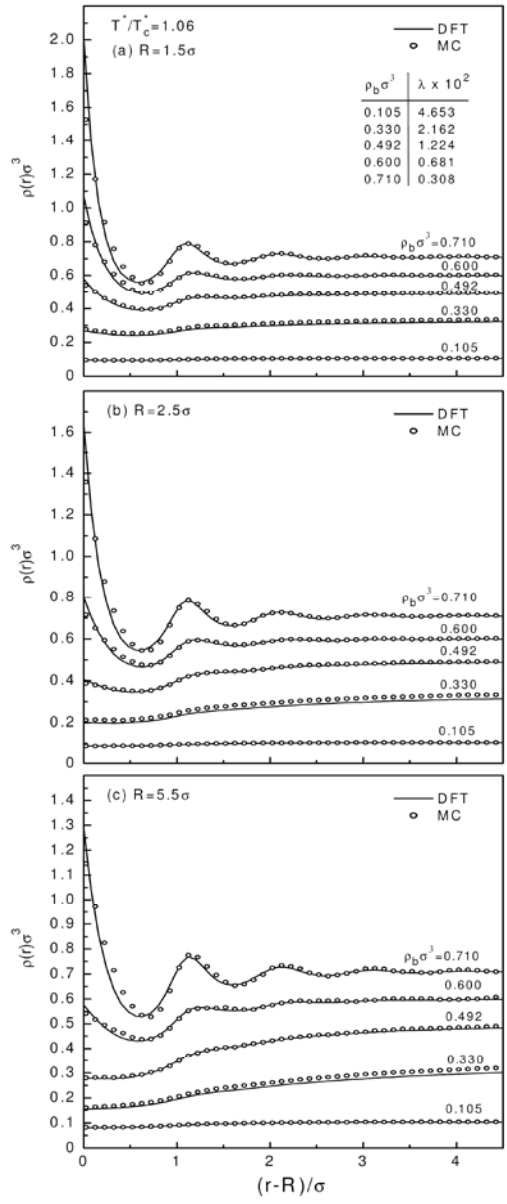

Figure 1. Monte Carlo (symbols) and density functional (lines) results for the density profiles of the LJ fluid near a large spherical particle of effective radius R = 1.5σ (a), R = 2.5σ (b), and R = 5.5σ (c), at the supercritical reduced temperature T^*/T_c^* = 1.06 and at different values of the bulk reduced density. λ is the adjustable parameter determined by the single hard wall sum rule considering the contact theorem using the exact simulation results for the contact densities.

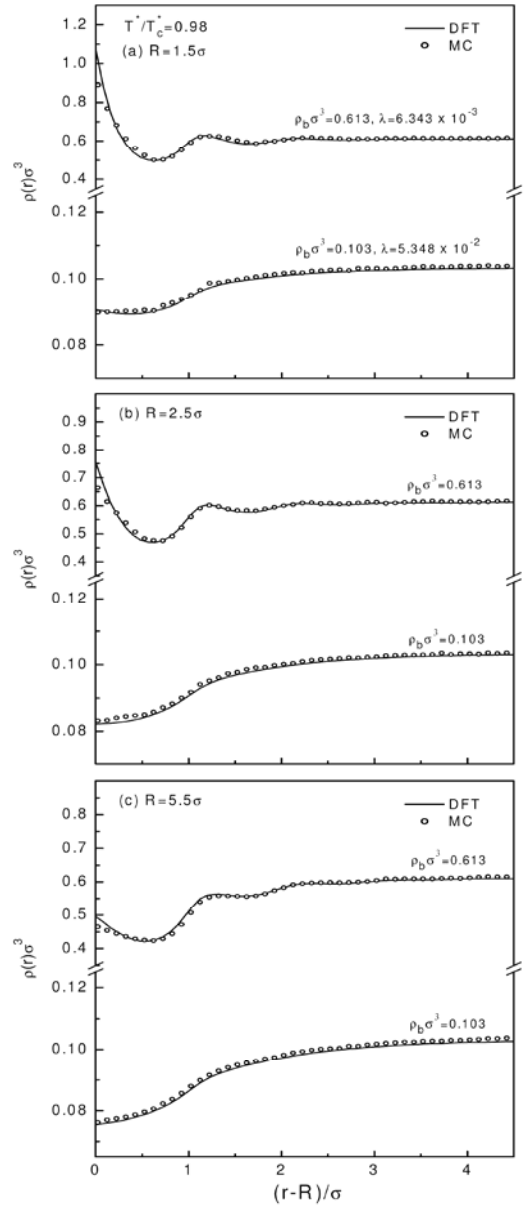

Figure 2. Monte Carlo (symbols) and density functional (lines) results for the density profiles of the LJ fluid near a large spherical particle of effective radius R = 1.5σ (a), R = 2.5σ (b), and R = 5.5σ (c), at the subcritical reduced temperature T^*/T_c^* = 0.98 and at two values of the bulk reduced densities: (i) $\rho_b\sigma^3$ = 0.103 (gaseous state) and (ii) $\rho_b\sigma^3$ = 0.613 (liquid state). λ is the adjustable parameter determined by the single hard wall sum rule considering the contact theorem using the exact simulation results for the contact densities.

in the limit of infinite macroparticle size resembling a flat single hard wall. At the supercritical temperature (Figure 1) it is interesting to observe somewhat larger deviations of the DFT results from the GCEMC data at intermediate bulk density approx. 0.3. This feature stem from the fact that this density corresponds to the condition of the bulk fluid lying in the most vicinity to the critical point.

A general observation following from the comparison between the theoretical DFT predictions and simulation data confirm the universality of the adjustable parameter λ, which is comprised in the DFT calculations. This means that it is independent on the external field responsible for the generation of the spatial inhomogeneous structure of the fluid. At a given set of bulk density and potential parameters, the

value of this parameter is determined by a single hard wall sum rule. The same value for λ is then used in the case of other external potentials.

4. Conclusions

In this paper we describe the general formalism of the third order+second order perturbation density functional approximation (DFA). The applicability of the DFA theory is demonstrated in the study of the structure of Lennard-Jones (LJ) fluid near a single large hard sphere of various sizes. The accuracy of DFA predictions is tested against the results of a grand canonical ensemble Monte Carlo simulation. The LJ fluid in this inhomogeneous system maintains equilibrium with the bulk LJ fluid, which is at the conditions situated at 'dangerous' regions of the phase diagram, i.e. the supercritical regions but near the critical temperature, or subcritical regions but close to the gas-liquid coexistence curve. The simulation data serve as a strict standard test for the validity of any density functional approximation (DFA), and concomitantly for the universality of the adjustable parameter, which is comprised in the DFA calculations. In this way, we found that the universality of this parameter holds also for the present inhomogeneous case. These results will also serve as a useful starting point for the further investigation of solvent-induced excess potential of mean force (PMF) in the similar systems. In a recently proposed framework[21] for the calculation of the solvent-induced excess PMF, the density profile of solvent particles around a single spherical solute particle represents important input information. For this reason, a theoretical method yielding sufficient and reliable results for this inhomogeneous fluid structure is significant for numerical implementation of the calculation framework.

5. Acknowledgements

Support from the Slovenian Research Agency through the grants Nos. P1-0201 and J1-6653 is appreciated. This project was supported also by the National Natural Science Foundation of China (Grants Nos. 20546004 and 20206033).

6. References

1. D. Henderson: Fundamentals of Inhomogeneous Fluids, Marcel Dekker, New York, **1992**.
2. J. L. Lebowitz, J. K. Percus, *J. Math.. Phys*. **1963**, *4*, 116–123; F. H. Stillinger, F. P. Buff, *J. Chem. Phys*. **1962**, *37*, 1–12; D. Mermin, *Phys. Rev. A* **1965**, *137*, 1441–1443.
3. P. Hohenberg, W. Kohn, *Phys. Rev. B* **1964**, *136*, 864–871; W. Kohn, L. J. Sham, *Phys. Rev. A* **1965**, *140*, 1133–1138.
4. T. V. Ramakrishnan, M. Yussouff, *Phys. Rev. B* **1979**, *19*, 2775–2794.
5. S. Zhou, E. Ruckenstein, *Phys. Rev. E* **2000**, *61*, 2704–2711.
6. S. Zhou, *New J. Phys*. **2002**, *4*, 36.
7. S. Zhou, *Phys. Lett. A* **2003**, *319*, 279–284.
8. P. Tarazona, *Phys. Rev. A* **1985**, *31*, 2672–2679.
9. Y. Rosenfeld, *Phys. Rev. Lett*. **1989**, *63*, 980–983.
10. S. Zhou, *J. Chem. Phys*. **2000**, *113*, 8719–8723.
11. S. Zhou, *J. Colloid and Interface Sci*. **2005**, *290*, 364–372; S. Zhou, *Int. J. Mod. Phys. B* **2005**, *19*, 4701–4721; S. Zhou, *Int. J. Mod. Phys. B* **2006**, *20*, 469–493; S. Zhou, *J. Chem. Phys*. **2006**, *accepted for publication*.
12. S. Zhou, *Commun. Theor. Phys*. (Beijing, China) **2003**, *40*, 721–726.
13. S. Zhou, A. Jamnik, *J. Chem. Phys*. **2005,** *122*, art. No. 064503.
14. S. Zhou, A. Jamnik, *Phys. Rev. E* **2006**, *73*, art. No. 011202.
15. D. Frenkel, B. Smit: Understanding Molecular Simulation, Academic Press, Boston, MA, **1996**.
16. J. J. Potoff, A. Z. Panagiotopoulos, *J. Chem. Phys*. **1998**, *109*, 10914–10920.
17. S. Zhou, *Phys. Rev. E* **2003**, *68*, art. No. 061201.
18. S. Zhou, *J. Chem. Phys*. **2004**, *121*, 895–901.
19. L. Verlet, *Mol. Phys*. **1980**, *41*, 183–190.
20. D. M. Duh, A. D. J. Haymet, *J. Chem. Phys*. **1995**, *103*, 2625–2633.
21. S. Zhou, *Chem. Phys. Lett*. **2004**, *392*, 110–115; S. Zhou, *Chem. Phys. Lett*. **2004**, *399*, 323–330; S. Zhou, *Chem. Phys. Lett*. **2004**, *399*, 315–322; S. Zhou, *J. Colloid and Interface Sci*. **2005**, *288*, 308–312; S. Zhou.Phys. Rev. E **2006**, *74*, art. No. 011402.

Povzetek

Opisane so osnovne značilnosti ene inačic teorije gostotnega funkcionala, to je perturbacijske teorije drugega in tretjega reda. Uporabnost te teorije smo preizkusili pri obravnavi strukture Lennard-Jones-ove (LJ) enostavne tekočine okoli velikih togih kroglic, ki ponazarjajo koloidne delce v disperziji. Zanesljivost teorijskih rezultatov smo preverili z računalniško simulacijo Monte Carlo odprtega sistema, ki omogoča obravnavo ravnotežja med nehomogenim in homogenim sistemom. Račune smo izvedli pri dveh temperaturah, ki sta bili le malo pod oz. nad kritično vrednostjo. Dobro ujemanje rezultatov obeh metod dokazuje, da je predlagana teorija zelo primerna za obravnavo strukturnih značilnosti nehomogenih sistemov. Rezultate bomo uporabili kot izhodišče za nadaljno obravnavo potenciala srednje sile med koloidnimi delci v sorodnih sistemih.